

**Supporting Information 1** Steady-state kinetic studies of the phosphorylation of LRRKtide catalyzed by wt LRRK2 (A) and the mutant G2019S (B). Initial velocities were measured as a function of LRRKtide at [ATP] = 500 (●), 250 (○), 125 (▼), 63 (▽), 31 (■), and 16  $\mu\text{M}$  (□)  $\mu\text{M}$ . Each data point is the average of duplicate determinations. Each data set was globally fit to the equation reflecting random mechanism.

**Supporting Information 2** Steady-state kinetic studies of the phosphorylation of PLK-peptide catalyzed by wt LRRK2 and the mutant G2019S. Initial velocities were measured as a function of [ATP] at [PLK-peptide] = 800 (●), 600 (○), 400 (▼), 200 (▽), 100 (■), 50 (□), and 25 (◆)  $\mu\text{M}$  for wt LRRK2 (A) and the mutant G2019S (B). Each data point is the average of duplicate determinations. The data set were globally fit to the equation reflecting random mechanism.

**Supporting Information 3** Steady-state kinetic studies of the phosphorylation of LRRKtide<sup>S</sup> catalyzed by wt LRRK2 and the mutant G2019S. Initial velocities were measured as a function of [LRRKtide<sup>S</sup>] at [ATP] = 500 (●), 250 (○), 125 (▼), 63 (▽), 31 (■), and 16  $\mu\text{M}$  (□) for wt LRRK2 (A) and the mutant G2019S (B). Each data point is the average of duplicate determinations. The data sets were globally fit to the equation reflecting random mechanism.

**Supporting Information 4** Isotope exchange analysis for tG2019S-catalyzed LRRKtide phosphorylation as a function of time. Examples of exchange of radioactive ATP to PO<sub>4</sub>-LRRKtide as a function of time under conditions of varied ADP/ATP (A), PO<sub>4</sub>-LRRKtide/ATP (B), ADP/LRRKtdie (C), and PO<sub>4</sub>-LRRKtide/LRRKtide (D). The concentrations of the varied reactants were maintained at a constant ratio of 20 while the other reactants were kept at 1 and 20  $\mu\text{M}$  for the substrate and product, respectively.

**Supporting Information 5** Isotope exchange analysis for tG2019S-catalyzed LRRKtide phosphorylation as a function of enzyme concentration. An example of initial exchange rate as a function of enzyme concentration under condition of varied  $\text{PO}_4\text{-LRRKtide/LRRKtide}$  while the concentration of ATP and ADP was kept at 1 and 20  $\mu\text{M}$ , respectively.

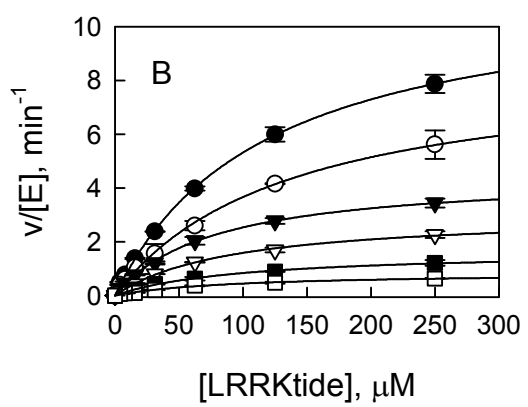
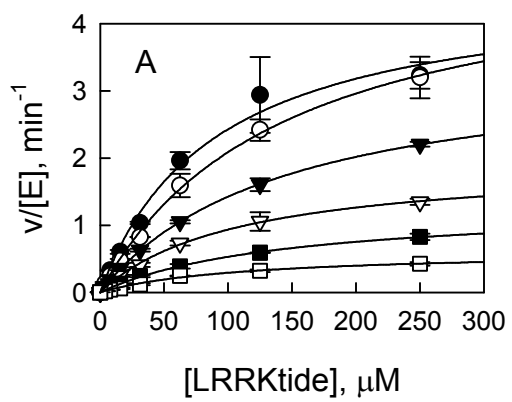
**Supporting Information 6** Inhibition study of the mutant G2019S-catalyzed phosphorylation of LRRKtide by products ADP and  $\text{PO}_4\text{-LRRKtide}$ . A: Plot of initial velocities vs [LRRKtide] at [ADP] = 500 ( $\bullet$ ), 250 (o), 125 ( $\blacktriangledown$ ), 31 ( $\blacksquare$ ), and 0  $\mu\text{M}$  ( $\square$ ) all at a fixed ATP concentration of 100  $\mu\text{M}$ . B & C: ADP concentration dependencies of  $(k_{\text{cat}})_{\text{LRRKtide}}$  and  $(k_{\text{cat}}/K_{\text{m}})_{\text{LRRKtide}}$  apparent values derived from analysis of the data of panel A. D: Plot of initial velocities vs [ATP] at [ $\text{PO}_4\text{-LRRKtide}$ ] = 2.5 ( $\bullet$ ), 1.3 (o), 0.6 ( $\blacktriangledown$ ), 0.2 ( $\blacksquare$ ), and 0 ( $\square$ ) mM all at a fixed LRRKtide concentration of 100  $\mu\text{M}$ . E & F:  $\text{PO}_4\text{-LRRKtide}$  concentration dependencies of  $(k_{\text{cat}})_{\text{ATP}}$  and  $(k_{\text{cat}}/K_{\text{m}})_{\text{ATP}}$  apparent values derived from analysis of the data of panel D.

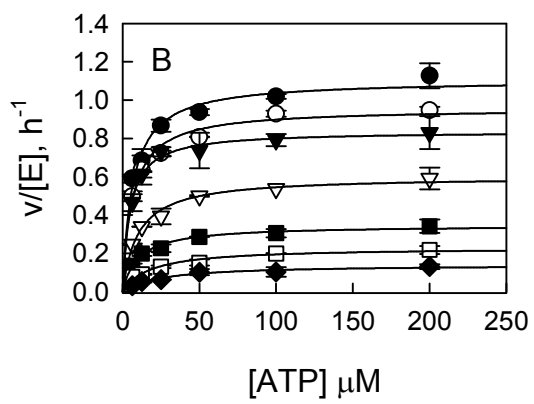
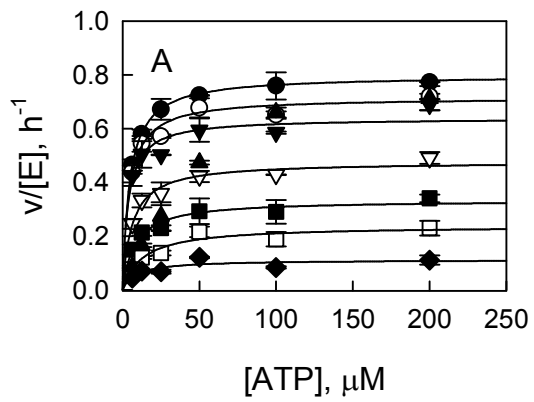
**Supporting Information 7** pL-dependence of steady-state kinetic parameters of the mutant G2019S-catalyzed LRRKtide<sup>S</sup> phosphorylation. A. pH ( $\bullet$ ) and pD (o) dependence of  $k_{\text{cat}}$  revealed an inverse SKIE of 0.65. B. pH ( $\bullet$ ) and pD (o) dependence of  $k_{\text{cat}}/K_{\text{m}}$  revealed an inverse SKIE of 0.56.

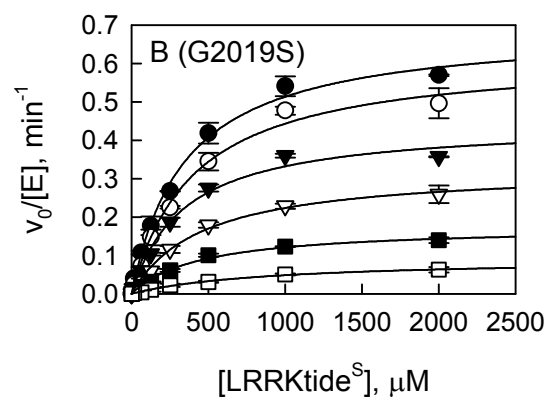
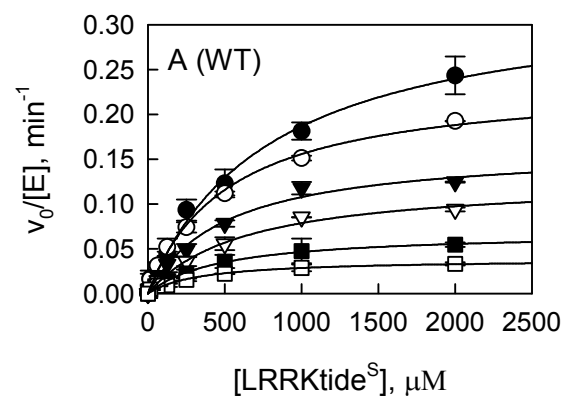
**Supporting Information 8** pL-dependence of steady-state kinetic parameters of the mutant G2019S-catalyzed LRRKtide phosphorylation. A. pH ( $\bullet$ ) and pD (o) dependence of  $k_{\text{cat}}$  revealed a SKIE of 1.1. B. pH ( $\bullet$ ) and pD (o) dependence of  $k_{\text{cat}}/K_{\text{m}}$  revealed a SKIE of 1. **Supporting information 9** (a) Homology model of the kinase domain of LRRK2 between residues 1885-2138. (b) Conserved domains within this family of

kinases shown with overall surface representation of the LRRK2 kinase domain. (c) Structural details of the ATP binding site showing the Glycine rich loop,  $Mg^{2+}$  atom and docked ATP molecule. D2017 from the DYG loop is shown to coordinate  $Mg^{2+}$  and ATP in the DYG-in conformation. (d) Two spatially conserved hydrophobic spines in LRRK2 are shown overlaid with other kinases where these conserved domains have been observed. These include PKA, b-RAF, c-Abl kinases.

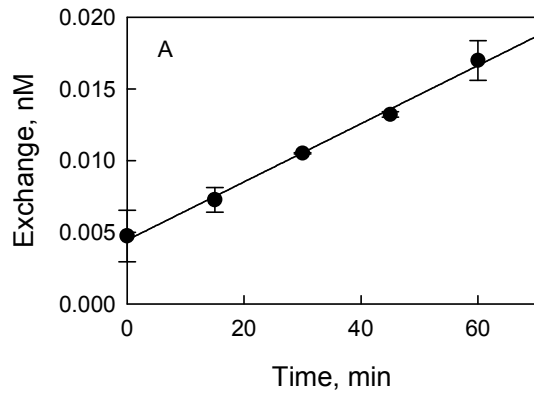
**Supporting information Figure 10** (a) Superposition of LRRK2 model with PKA and their respective substrates. (b) calculated electrostatic potential (red and blue represent electrostatic potentials  $<-9$  and  $>+9$  kBT, respectively, where kB is the Boltzmann constant and T is the absolute temperature). LRRK2 is shown as stick representation.



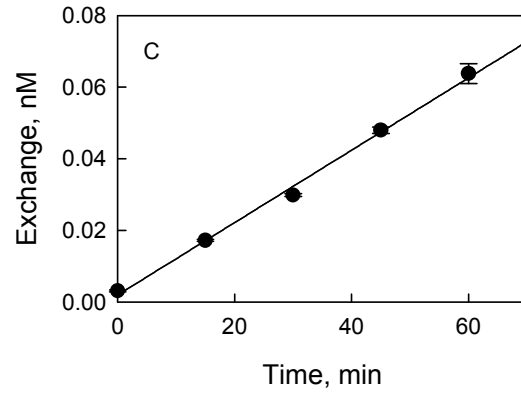




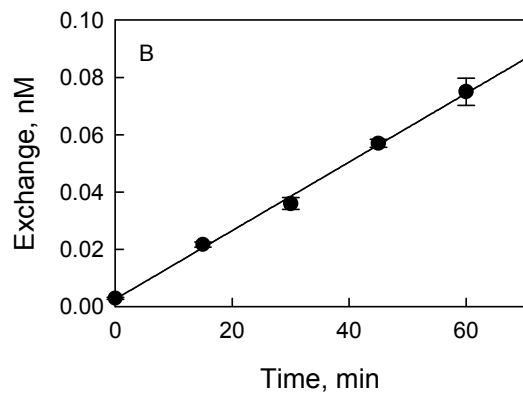
Vary ADP/ATP



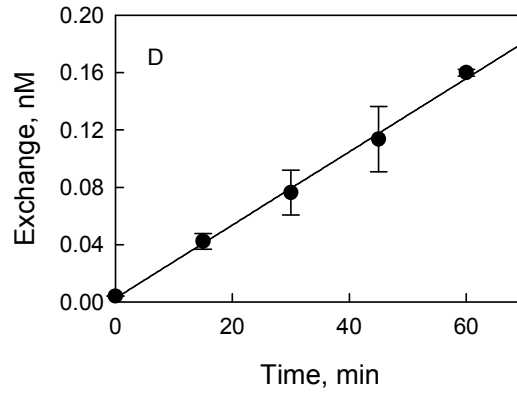
Vary ADP/LRRKtide

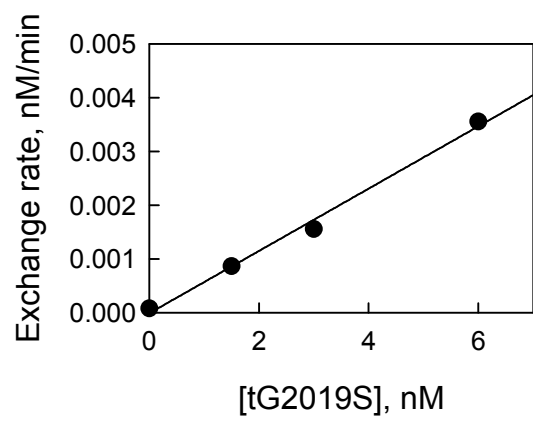


Vary  $\text{PO}_4$ -LRRKtide/ATP

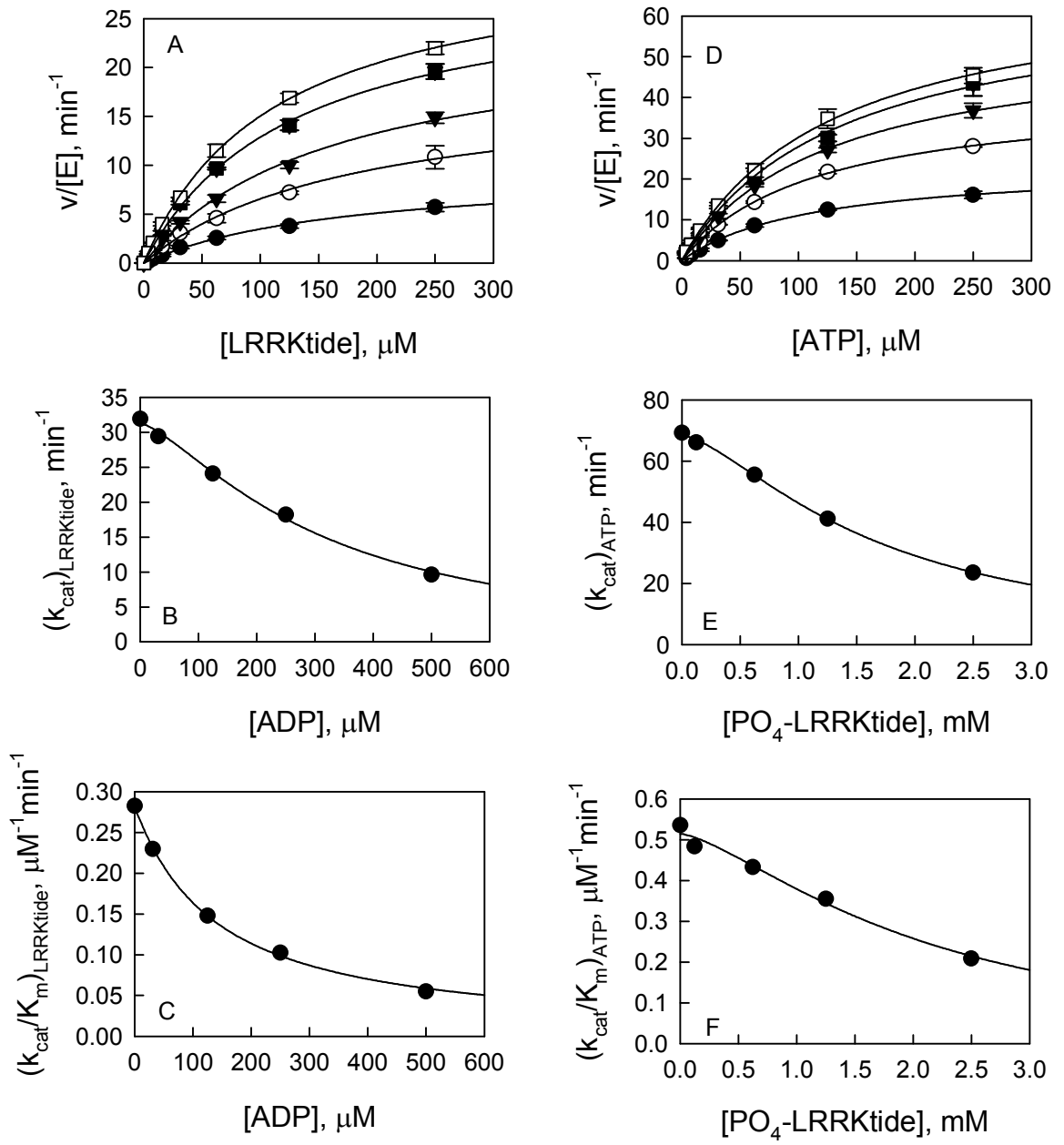


Vary  $\text{PO}_4$ -LRRKtide/LRRKtide









Supporting Information 6

